Solar Energy Materials & Solar Cells 93 (2009) 1932–1938

Contents lists available at ScienceDirect

Solar Energy Materials & Solar Cells

journal homepage: www.elsevier.com/locate/solmat

Synthesis and characterization of 2,1,3-benzothiadiazole-thieno[3,2-b] thiophene-based charge transferred-type polymers for photovoltaic application

Jang Yong Lee [a], Soo Won Heo [a], Heelack Choi [b], Yoon Jung Kwon [c], Jung Rim Haw [a], Doo Kyung Moon [a,*]

[a] Department of Materials Chemistry and Engineering, Konkuk University, 1 Hwayang-dong, Gwangjin-Gu, Seoul 143-701, South Korea
[b] Department of Materials Science and Engineering, Pukyong National University, san 100 YongDang-Dong, Nam-Gu, Busan 608-739, South Korea
[c] Department of Textile Engineering, Konkuk University, 1 Hwayang-dong, Gwangjin-Gu, Seoul 143-701, South Korea

ARTICLE INFO

Article history:
Received 2 March 2009
Received in revised form
7 July 2009
Accepted 8 July 2009
Available online 6 August 2009

Keywords:
Organic photovoltaics
Donor materials
Bulk heterojunction
Thieno[3
2-b]thiophene
2,1,3-benzothiadiazole

ABSTRACT

New low-band-gap copolymers, including thieno[3,2-b]thiophene and 2,1,3-benzothiadiazole, were synthesized as photovoltaic materials. Thiophene was introduced to provide extended π-conjugation length and charge transfer properties. A band gap ($E_g^{op} = 1.62$ eV, $E_g^{ec} = 1.51$ eV) of this polymer was investigated through UV–vis spectroscopy and cyclic voltammetry. A bulk heterojunction structure of glass/indium tin oxide (ITO)/PEDOT:PSS/polymer-PCBM(1:3)/LiF/Al was fabricated for investigating photovoltaic properties. $PC_{71}BM$ was used as an acceptor material, due to its increased absorption in the visible region, in comparison with $PC_{61}BM$. In this polymer, incident photon-to-current conversion efficiency (IPCE) was as high as 50%. Moreover, maximum power conversion efficiency (PCE) of up to 1.72% was achieved under AM 1.5 G conditions. It demonstrated relatively high V_{OC} (0.67 V) and J_{SC} (6.86 mA/cm^2), while a low fill factor value (0.37) was obtained.

1. Introduction

Various aromatic ring-based conjugated polymers have been developed for use in potential applications, such as organic light-emitting diodes (OLEDs) [1,2], organic thin-film transistors (OTFTs) [3,4], and organic photovoltaics (OPVs) [5–7]. In particular, OPVs have generated considerable scientific interest due to a potential in fabricating low-cost integrated circuit elements for large area and the feasibility of low production using various methods such as spin coating, ink-jet printing, and roll-to-roll through solution process [8–11]. One of the most efficient donor components to date has been the semiconducting polymer poly(3-hexylthiophene) (P3HT) in combination with a soluble fullerene derivative as the nonpolymeric acceptor. However, the maximum power conversion efficiency (PCE) of this donor–acceptor (DA) couple is limited to ~5% due to incomplete match with the solar spectrum and the large offset of lowest unoccupied molecular orbital (LUMO) energy levels of the DA [12–14]. Therefore, the development of low-band-gap polymers, having a better overlap with the solar spectrum, is needed for maximum photon harvesting in OPV devices [15–18].

Recently, low-band-gap polymers have been developed to better match the solar output, which has a maximum photon flux near 700 nm and an appreciable tail stretching into the infra-red region [19]. The typical ways to lower band gap in polymerization are to improve intermolecular interaction and to increase π-conjugation length [20]. However, it is not easy to reduce the band gap extensively throughout by these methods, because it is hard to control the polymer structure by increasing conjugated repeating units. The introduction of electron-rich and electron-poor building blocks into the polymer backbone is regarded as a more powerful and efficient method to synthesize low-band-gap polymers, as alternating donor–acceptor units lower the effective band gap by orbital mixing [21–23]. In DA-type polymers, the high energy level for the highest occupied molecular orbital (HOMO) of the donor and the low energy level for the LUMO of the acceptor results in a low band gap due to an intra-chain charge transfer from donor to acceptor [24–27]. In principle, if donor polymers having a well-aligned energy level, an outstanding charge transport property, and low band gap that could harvest photons in the range of the infra-red region were to be developed, the performance of bulk heterojunction-type solar cells with an active layer of these DA-type copolymers and [6,6]-phenyl-C_{61}-butyric acid methyl ester (PCBM) could reach 10% PCE [14].

In this study, new CT-type copolymers, based on 2,1,3-benzothiadiazole-thieno[3,2-b]thiophene, poly[2,5-bis(thieno-2-yl)

* Corresponding author. Tel.: +82 2 450 3498; fax: +82 2 444 0765.
E-mail address: dkmoon@konkuk.ac.kr (D.K. Moon).

0927-0248/$ - see front matter © 2009 Elsevier B.V. All rights reserved.
doi:10.1016/j.solmat.2009.07.006

-3,6-dipentadecylthieno[3,2-b]thiophene-co-2,1,3-benzothiadiazole] (**P1**), and poly[2,5-bis(3,4-ethylenedioxythieno-2-yl)-3,6-dipentadecylthieno[3,2-b]thiophene-co-2,1,3-benzothiadiazole] (**P2**), were synthesized through the Stille coupling reaction for OPVs. Thiophene and 3,4-ethylenedioxythiophene molecules were introduced into the polymer backbone to increase the charge transporting property and π-conjugation length [28]. Because of their high electron-accepting and good planarity, 2,1,3-benzothiadiazole and thieno[3,2-b]thiophene, respectively, are extensively used in the chemistry of organic electronics. Moreover, a polymer that contains 2,5-bis(2-thienyl)-3,6-dialkylthieno[3,2-b]thiophene moiety in a polymer chain has good stacking property and charge transporting ability. Devices (indium tin oxide (ITO)/PEDOT:PSS/pol:PCBM/LiF(7 Å)/Al(120 nm)) were fabricated to measure the photovoltaic properties.

2. Experimental

2.1. Materials

All reagents and chemicals were purchased from Aldrich. Chloroform was dried over $CaCl_2$ and THF. Toluene was dried over sodium/benzophenone under a nitrogen atmosphere. Other reagents and chemicals were used as received; 2-(trimethylstannyl)thiophene, 2-(trimethylstannyl)-3,4-ethylenedioxythiophene, 4,7-dibromo-2,1,3-benzothiadiazole, and 2,5-dibromo-3,6-dipentadecynylthieno[3,2-b]thiophene—**1** were prepared as described in the literatures [29–32].

2.2. Instruments

^{1}H NMR spectra were performed in a Brüker ARX 400 spectrometer using solutions in $CDCl_3$ and chemicals were recorded in ppm units with TMS as the internal standard. The UV–vis spectra were measured with a HP Agilent 8453 UV–vis. All gel permeation chromatography (GPC) analyses were made using THF as eluent and polystyrene standard as reference. Cyclic voltammetric waves were produced using a Wonatech WMPG 1000 with a 0.1 M acetonitrile (substituted a nitrogen in 20 min) solution containing tetrabutylammonium tetrafluoro borate (TBABF4, Fluka 99.9%) at a constant scan rate of 50 mV/s. The working electrode (WE) and the counter electrode (CE) were platinum plates. A silver wire coated with AgCl was used as the reference electrode (RE). After each measurement, the RE was calibrated with ferrocene. Current density–voltage (*J–V*) characteristics of all polymer photovoltaic cells were measured under the illumination of simulated solar light with 100 mW/cm^2 (AM 1.5 G) by Oriel 1000 W solar simulator. Electric data were recorded using a Keithley 236 source-measure unit and all characterizations were carried out in an ambient environment. The illumination intensity used was calibrated by a standard Si photodiode detector from Bunkoukeiki Co., Ltd. The incident photon-to-current conversion efficiency (IPCE) was measured as a function of wavelength from 360 to 800 nm (PV measurement Inc.) equipped with a halogen lamp as a light source, and calibration was performed using a silicon reference photodiode. Thickness of the thin film was measured using a KLA Tencor Alpha-step 500 surface profilometer with an accuracy of 1 nm.

2.3. Synthesis

2.3.1. 2,5-bis(2-thienyl)-3,6-dipentadecylthieno[3,2-b]thiophene—2

To a mixture of **1** (2 g, 2.77 mmol) and 2-(trimethylstannyl)thiophene (1.64 g, 6.66 mmol) were added bis(triphenylphosphine)palladium(α)dichloride (97 mg, 0.14 mmol) and anhydrous THF (20 mL). The reaction flask was evacuated and then filled with argon several times, after which the reaction mixture was refluxed for 12 h. The reaction mixture was cooled to room temperature and was then poured into deionized water. $CHCl_3$ was added to extract the product from the aqueous layer, and the combined organic layers were washed with water and brine. The organic layer was dried over anhydrous Na_2SO_4, and the solvent was removed by rotary evaporation. The residue was purified by column chromatography (silica gel, 30% EA in hexane) to provide 1.2 g (60%) product **2** as a yellow solid. ^{1}H NMR ($CDCl_3$, 400 MHz) *d* (ppm): 7.34 (d, $J = 4.9$ Hz, 2H), 7.16 (d, $J = 2.6$ Hz, 2H), 7.09(t, $J1 = 4.9$ Hz, 2H), 2.87 (t, $J = 7.9$ Hz, 4H), 1.76 (m, 4H), 1.25–1.40 (m, 48H), 0.88 (t, $J = 6.5$ Hz, 6H).

2.3.2. 2,5-bis(5-trimethylstannyl-thienyl-2yl)-3,6-dipentadecylthieno[3,2-b]thiophene—3

To a mixture of **2** (0.91 g, 1.25mmol) in anhydrous THF (15 mL) at −25 °C was added 1.6 mL n-butyllithium (1.6 M in hexane) by syringe. The mixture was stirred at −25 °C for 1 h. Trimethylstannylchloride was added dropwise to the solution, and resulting mixture was warmed to room temperature and stirred for 24 h. The mixture was poured into water and extracted with chloroform. The organic extracts were washed with brine and dried over anhydrous Na_2SO_4. The solvent was removed by rotary evaporation and the crude product was obtained as a yellow solid (1 g, 76%). It was used directly in the next step without further purification. ^{1}H NMR ($CDCl_3$, 400 MHz) *d* [ppm]: 7.29 (d, $J = 2.6$ Hz, 2H), 7.15(d, $J1 = 4.9$ Hz, 2H), 2.87 (t, $J = 7.9$ Hz, 4H), 1.76 (m, 4H), 1.25–1.40 (m, 48H), 0.88 (t, $J = 6.5$ Hz, 6H), 0.43 (s, 18H).

2.3.3. 2,5-bis(3,4-ethylenedioxithieno-2-yl)-3,6-dipentadecylthieno[3,2-b]thiophene—4

Prepared as above for compound **2**. Yield: 56%, yellow solid. ^{1}H NMR ($CDCl_3$, 400 MHz) *d* (ppm): 6.39 (s, 2H), 4.27 (d, $J = 2.6$ Hz, 8H), 2.78 (t, $J = 7.9$ Hz, 4H), 1.71 (m, 4H), 1.24–1.35 (m, 48H), 0.87 (t, $J = 6.5$ Hz, 6H).

2.3.4. 2,5-bis(5-tri-n-methylstannyl-3,4-ethylenedioxithieno-2-yl)-3,6-dipentadecylthieno[3,2-b]thiophene—5

Prepared as above for compound **3**. Yield: 81%, yellow solid. ^{1}H NMR ($CDCl_3$, 400 MHz) *d* (ppm): 4.27 (d, $J = 2.6$ Hz, 8H), 2.78 (t, $J = 7.9$ Hz, 4H), 1.71 (m, 4H), 1.24–1.35 (m, 48H), 0.87 (t, $J = 6.5$ Hz, 6H), 0.38 (s, 18H).

2.3.5. Poly[2,5-bis(thieno-2-yl)-3,6-dipentadecylthieno[3,2-b]thiophene-co-2,1,3-benzothiadiazole]—***P1***

Compounds **3** (0.5 g, 0.476mmol) and 4,7-dibromo-2,1,3-benzothiadiazole (0.14 g, 0.476mmol) were dissolved in toluene (15 mL) under nitrogen atmosphere. $Pd(PPh_3)Cl_2$ (1.0 mol%) was dissolved in the mixture and vigorously stirred for 10 min. The mixture was stirred at 85–90 °C for 48 h under nitrogen. After the mixture was cooled to room temperature, it was poured into methanol. A powder obtained by filtration was reprecipitated with methanol several times. The polymer was further purified by washing with methanol, acetone, and hexane in a Soxhlet apparatus for 24 h and dried under reduced pressure at 50 °C. Dark violet solid 0.2 g (yield 49%). ^{1}H NMR ($CDCl_3$, 400 MHz) *d* [ppm]: 7.70 (d, 2H), 7.58 (d, 2H), 7.54 (s, 2H), 7.25 (s, 2H), 7.10 (d, 2H), 7.05 (d, 2H), 2.63 (t, 4H), 1.94 (t, 4H), 1.58 (m, 4H), 1.24 (m, 20H), 1.18 (m, 4H), 1.05 (m, 20H), 0.86 (t, 6H), 0.80 (t, 6H).

*2.3.6. Poly[2,5-bis(3,4-ethylenedioxythieno-2-yl)-3,6-dipentadecylthieno[3,2-b]thiophene-co-2,1,3-benzothiadiazole]—**P2***

Prepared as above for **P1**. Dark violet solid 0.17 g (yield 46.7%). ^{1}H NMR ($CDCl_3$, 400 MHz) *d* (ppm): 8.47 (s, 2H), 8.28 (d, 0.5H), 7.85 (d, 0.5H), 6.40 (s, 0.25H), 4.45 (d, 8H), 2.82 (t, 4H), 2.63 (t, 4H), 1.44–1.21(m, 48H), 0.85 (t, 6H).

2.4. Device fabrication

Composite solutions with polymers and PCBM were prepared using 1,2-dichlorobenzene (DCB). The concentration was controlled adequately in a range of 1.0–2.0 wt%. The polymer photovoltaic devices were fabricated with a typical sandwich structure of ITO/PEDOT:PSS/active layer/LiF/Al. The ITO-coated glass substrates were cleaned through a routine cleaning procedure, including sonication in detergent followed by distilled water, acetone, and 2-propanol. A 45 nm thick layer of PEDOT:PSS (Baytron P) was spin coated on a cleaned ITO substrate after exposing the ITO surface to ozone for 10 min. The PEDOT:PSS layer is baked on a hot plate at 120 °C for 10 min. The active layer was spin coated from the pre-dissolved composite solution after filtering through 0.45 μm poly(tetrafluoroethylene) (PTFE) syringe filters. The resulting films were thermally treated at 120 °C for 5 min before deposition on the electrode. The device structure was completed by depositing 120 nm Al cathode as top electrode onto the polymer active layer under 3×10^{-6} Torr vacuum in thermal evaporator.

3. Results and discussion

3.1. Synthesis of the monomers and polymers

Scheme 1 shows the syntheses of **P1** and **P2**. The synthesis of **1** was carried out according to procedures described previously. 2,5-Dibromo-3,6-dipentadecylthieno[3,2-b]thiophene—**1** was synthesized by bromination of 3,6-dipentadecylthieno[3,2-b]thiophene with NBS, and 2,5-bis(2-thienyl)-3,6-dipentadecylthieno[3,2-b]thiophene—**2** and 2,5-bis(3,4-ethylenedioxithieno-2-yl)-3,6-dipentadecylthieno[3,2-b]thiophene—**4** were obtained by Stille coupling reaction between **1** and 2-trimethylthiophene, 2-trimethyl-3,4-ethylenedioxythiophene, respectively. Compounds **3** and **5** were directly synthesized from compounds **2** and **4** without bromination. Because of the poor solubility and long chain length of compounds **2** and **4**, it was difficult to stannate them. The syntheses of **P1** and **P2** were accomplished by the copolymerization of compounds **3** and **5** with 4,7-dibromo-2,1,3-benzothiadiazole in the presence of $Pd(PPh_3)Cl_2$. Proton nuclear magnetic resonance (^{1}H NMR) data were consistent with the proposed structure of the polymers. The ^{1}H NMR peaks of the polymers were broader than the peaks of the monomers. The ^{1}H NMR spectrum of **P1** in $CDCl_3$ showed peaks indicating two protons of benzothiadiazole at $\delta = 8.15$ ppm and four protons of thiophene at $\delta = 7.70$ and 7.10 ppm. Protons of alkyl side chains of fused thiophene appeared between $\delta = 3.07$ and 0.82 ppm. Similarly, the ^{1}H NMR spectrum of **P2** in $CDCl_3$ showed peaks indicating protons of benzothiadiazole at $\delta = 8.47$ ppm. In the ^{1}H NMR spectrum of **P2**, two doublet peaks were observed at 8.28 and 7.85 ppm. It is assumed that these are peaks of protons of terminal 2,1,3-benzothiadiazole in polymer chains, originating from the low molecular weights of **P2**. Four protons of ethylenedioxythiophene were observed at $\delta = 4.43$ ppm, and protons of alkyl side chains of fused thiophene appeared between $\delta = 2.96$ and 0.82 ppm.

3.2. Molecular weight and thermal property

The average molecular weights of polymers were determined by gel permeation chromatography (GPC) with polystyrene as the standard. Tetrahydrofuran (THF) served as the eluting solvent. The number-average molecular weight (Mn) values of **P1** and **P2** were 6815 and 2872, and the weight-average molecular weight (Mw) values of **P1** and **P2** were 17215 and 4875, respectively. The molecular weights of the polymers were not high. Most notably, **P2** had a very low molecular weight. This low value indicated that **P2** had three or four repeating moieties, stemming from poor solubility of the 3,4-ethylenedioxythiophene units.

The thermal properties of these copolymers were investigated using thermogravimetric analysis (TGA) at a heating rate of 10 K/min. **P1** and **P2** had decomposition temperatures (T_d) of 343 and 360 °C, respectively. The values indicate that these polymers have good thermal stability, making them applicable for use in

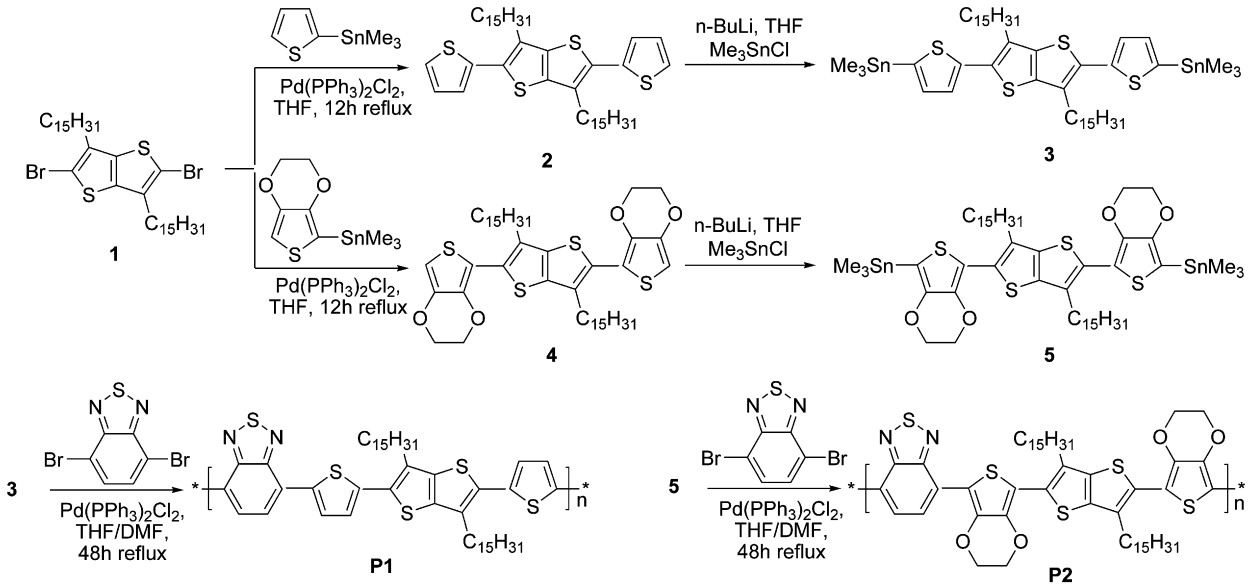

Scheme 1. Synthesis routes of poly[2,5-bis(thieno-2-yl)-3,6-dipentadecylthieno[3,2-b]thiophene-co-2,1,3-benzothiadiazole] and poly[2,5-bis(3,4-ethylenedioxythieno-2-yl)-3,6-dipentadecylthieno[3,2-b]thiophene-co-2,1,3-benzothiadiazole].

Table 1
Molecular weights and thermal properties of the two polymers.

Polymer	Yield (%)	M_n[a]	M_w[a]	PDI	T_d[b] (°C)
P1	49	6815	17,215	2.5	343
P2	46.7	2872	4835	1.7	360

[a] Molecular weights and ploydispersity indexes determined by GPC in THF on the basis of polystyrene calibration.
[b] T_g measured by TGA under N2.

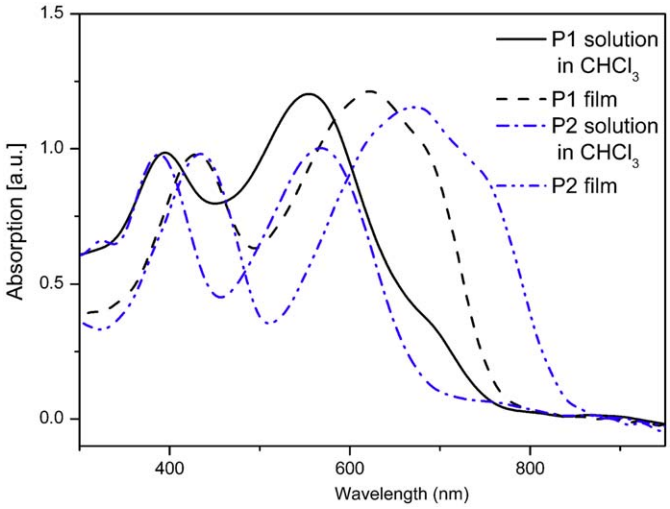

Fig. 1. Comparison of UV–vis absorption spectra of **P1**, **P2** in chloroform solution and solid state.

Table 2
UV-–vis data for **P1**, **P2** in dilute chloroform solution and the thin film.

Polymer	Absorption λ_{max} (nm)[a]		E_g^{op}(eV)[c]
	In $CHCl_3$	In film[b]	
P1	394, 554	432, 624, 678 (shoulder)	1.62
P2	386, 570	436, 674, 738 (shoulder)	1.48

[a] λ_{max} was determined from UV-–vis data.
[b] Spin- coated from a chloroform.
[c] Estimated from the onset absorption of the thin film.

Table 3
Electrochemical data of polymers as obtained from cyclic voltammetry and electrochemical voltage spectroscopy.

Polymer	Oxidation potential (V)		Reduction potential (V)		Energy level[e] (eV)		$E_g^{e,c,f}$ (eV)
	E_{ox}[a]	$E_{onset,\ ox}$[b]	E_{red}[c]	$E_{onset,\ red}$[d]	HOMO	LUMO	
P1	1.13	0.73	−1.17	−0.73	−5.17	−3.66	1.51
P2	0.97	0.56	−1.25	−0.96	−5	−3.48	1.52

All potentials are given vs. Ag/AgCl electrode.

[a] Final oxidation potential.
[b] Onset oxidation potential.
[c] Final reduction potential.
[d] Onset reduction potential.
[e] Calculated from the reduction and oxidation potentials under the assumption that the absolute energy level of Fc/Fc+ was 4.8 eV below a vacuum.
[f] Band gaps drivedderived from the difference between onset potentials of oxidation and reduction.

polymer solar cells and other optoelectronic devices. The molecular weights and thermal properties of **P1** and **P2** are shown in Table 1.

3.3. Optical and electrochemical measurements

Fig. 1 shows the normalized UV–vis absorption of the polymers in chloroform solution and in thin solid films. Two distinct absorption bands are observed. **P1** and **P2** display similar maximum absorption wavelength values (394 and 554 and 386 and 570 nm, respectively) in $CHCl_3$ solution. The λ_{max} values of **P1** and **P2** in the solid film were red shifted by approximately 70 and 100 nm, respectively. **P2** was more red shifted than **P1** owing to the stronger electron-donating property of 3,4-ethylenedioxythiophene units than of thiophene. Shoulder peaks were observed at 678 nm (**P1**) and 738 nm (**P2**), indicating that these polymers have good intermolecular interaction [33,34]. The optical band gaps calculated from the band edge of **P1** and **P2** were 1.62 and 1.48 eV, respectively. Maximal wavelengths of the absorption peaks and optical band gaps of the polymers are summarized in Table 2.

Electrochemical behaviors of the copolymers were investigated by cyclic voltammetry (CV). The supporting electrolyte was tetrabutylammonium hexafluorophosphate ($TBAPF_6$) in acetonitrile (0.1 M) at a scan rate of 50 mV/s. A three-electrode cell was used and silver/silver chloride [Ag in 0.1 M KCl] was used as a RE. Onset potentials are values obtained from the intersection of the two tangents drawn at the rising current and the baseline changing current of the CV curves. The onset and the peak potentials, the electrochemical band gap energy, and the estimated position of the upper edge of the valence band (HOMO) and of the lower edge of conduction band (LUMO) are listed in Table 3.

As shown by the cyclic voltammograms in Fig. 2, the electrochemical oxidation of **P1** starts at 0.73 V vs. Ag/AgCl and gives a p-doping peak at 1.13 V vs. Ag/AgCl. The oxidation of **P2** starts at 0.56 V vs. Ag/AgCl and gives a p-doping peak at 0.97 V vs. Ag/AgCl. Similarly, the reduction of **P1** and **P2** starts at −0.73 and −0.96 V vs. Ag/AgCl and gives an n-doping peak at −1.17 and −1.25 V vs. Ag/AgCl, respectively. In the range of 2.0 to −2.0 V vs. Ag/AgCl, the films of **P1** and **P2** revealed stability in repeated scanning by CV. However, the thin films decomposed over 2.0 V vs. Ag/AgCl and below −2.0 V vs. Ag/AgCl. Electrochemical band gap energy was directly measured from the CV. Several methods to evaluate HOMO and LUMO energy levels from the onset potentials have been proposed in the literature [35,36]. The levels were estimated here on the basis of the reference energy level of ferrocene (4.8 eV below the vacuum level) [37,38], according to the following equation:

$$E^{HOMO/LUMO} = [-(E_{onset}\ (\text{vs. Ag/AgCl}) - E_{onset}\ (Fc/Fc^{+}\ \text{vs. Ag/AgCl})] - 4.8\ \text{eV}$$

According to this equation, HOMO levels of **P1** and **P2** were −5.17 and −5.0 eV and the LUMO levels of **P1** and **P2** were −3.66 and −3.48 eV, respectively. The high HOMO level of **P2** is followed by strong electron donor properties of the 3,4-etylenedioxythiophene(EDOT) unit. This can give rise to noncovalent intermolecular interactions with adjacent thiophenic units, thus inducing self-rigidification of the π-conjugated system in which it is incorporated [39]. The electrochemical band gaps, estimated from the HOMO and LUMO of **P1** and **P2**, were 1.51 and 1.52 eV, which are close to optical band gap energy levels. Normally, the E_g^{ec} are higher than E_g^{op}. Differences between E_g^{op} and E_g^{ec} reflect the fact that free ions are created in the electrochemical experiment rather than a neutral excited state [40]. However, the E_g^{ec} of **P1** was

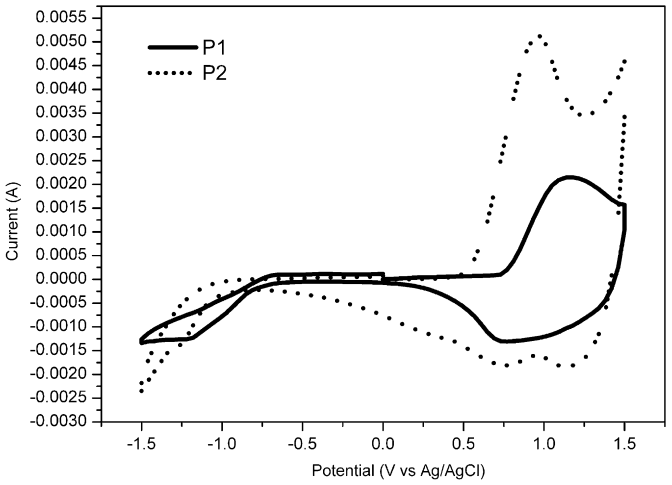

Fig. 2. Cyclic voltammograms of thin films recorded in 0.1 M $TBAPF_6$/acetonitrile at a scan rate of 50 mV/s.

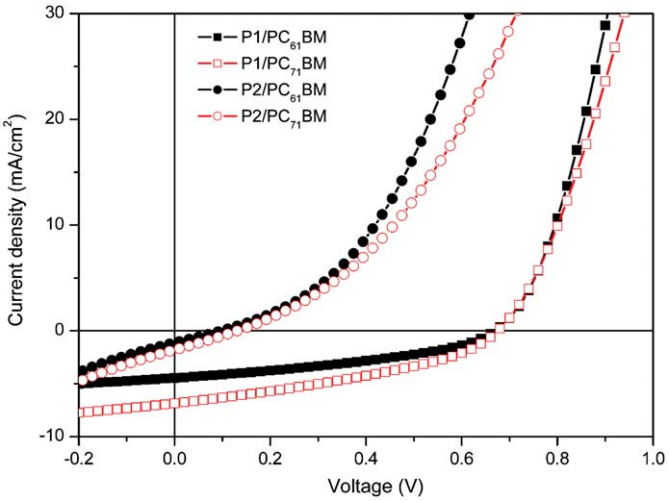

Fig. 3. *I–V* characteristics of photovoltaic devices made from **P1**, **P2** and their mixture in the ratio of 1:3 (by weight) blended with $PC_{61}BM$ and $PC_{71}BM$.

smaller than the E_g^{op}. As shown in Fig. 2, It seems that unstable reduction state of thiophene unit of **P1** results in nuclear reduction potential [41,42].

3.4. Photovoltaic studies

The polymer materials were all applied in bulk heterojunction geometry (BHG) with PCBM. OPV cells, with the sandwiched structure of glass/ITO/PEDOT:PSS/polymer-PCBM(1:3)/LiF/aluminium, were fabricated. Each substrate was patterned using photolithography techniques to produce a segment with an active area of 9.0 mm^2. Prior to use, the substrates were cleaned with detergent and deionized water. Thereafter, ultrasonication in deionized water and isopropanol was performed. PEDOT:PSS (Baytron P) was spin coated on an indium tin oxide slide and dried at 120 °C for 10 min. A blend of polymer and $PC_{71}BM$ was solubilized overnight in DCB, filtered through a 0.45 μm poly (tetrafluoroethylene) (PTFE) filter, and spin coated. The active layers were pre-annealed at 120 °C for 5 min before deposition on the electrode. The devices were completed by deposition on 7 Å LiF and 120 nm aluminium layers as an electrode. Current vs. potential curves (*I–V* characteristics) were measured with a Keithley 2400 Digital Source Meter. Illumination of the cells was done via the ITO side using light from a 150 W Oriel Instruments Solar Simulator and xenon lamp using an AM 1.5 G filter. All fabrications and characterizations were performed in an ambient environment without a protective atmosphere.

A typical *I–V* curve of **P1** and **P2**, demonstrating the behavior of the device, is presented in Fig. 3. Devices having various active layer thicknesses were fabricated to optimize the photovoltaic property. When $PC_{71}BM$ was introduced as an acceptor, the PCE of **P2** was as low as 0.045%. However, when tested under AM 1.5 G (100 mW/cm^2) solar illumination, **P1** photovoltaic cells, having an active layer 58 nm thick, regularly demonstrated PCEs of up to 1.72%. Even though the fill factor value was as low as 0.37, a good current density (6.86 mA/cm^2) and a relatively high open-circuit voltage, 0.67 V, were obtained.

In spite of a large absorption range, one reason of the low PCE value for **P2** is low molecular weight and solubility. M_w of **P2** was as low as 4835 and solubility of synthesized polymer was very low in organic solvent. A rigid structure of EDOT prevented **P2** from having a high molecular weight and good solubility, which hindered **P2**/PCBM blend films from having an effective photon

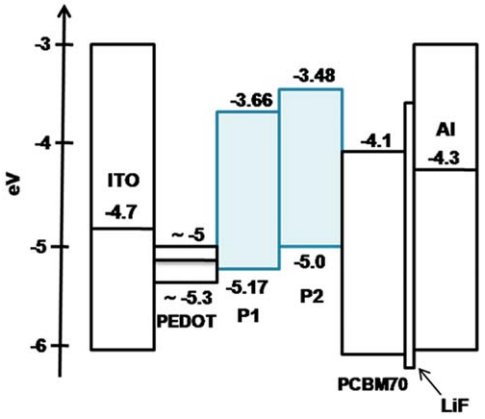

Fig. 4. Energy scheme for **P1**, **P2**/$PC_{71}BM$.

harvesting and charge transport properties. Another reason is unbalanced energy levels between the polymer and the acceptor, as shown in Fig. 4. A large LUMO energy value difference between the donor and acceptor allows for increased energy loss in photovoltaic devices. Moreover, the high HOMO level resulting from the strong electron donor properties of the EDOT molecules caused a reduction in the open-circuit voltage. Compared with **P2**, **P1** has a more balanced acceptor energy level.

To confirm the acceptor effect in the polymer/PCBM blend, $PC_{61}BM$ was introduced instead of $PC_{71}BM$ as an acceptor. The PCE of the devices with **P1**/$PC_{61}BM$ and **P2**/$PC_{61}BM$ blend film as an active layer was regularly 1.15% and 0.017%, respectively. In a device with the **P1**/$PC_{61}BM$ active layer, V_{OC} and FF of this device were as high as 0.67 V and 0.38, respectively, while the current density was decreased. A reduction of current density and PCE in the **P1**/$PC_{61}BM$ blend originates from the difference of IPCE values in the different blending systems. As shown in Fig. 5, the IPCE values obtained in the **P1**/$PC_{71}BM$ blend are considerably high at the main absorption peak (range 400–550 nm) and approach 49%, which shows that the system has the ability to efficiently convert photons into electrons in an external circuit. The onset of photocurrent starts at approximately 750 nm, in agreement with the optical data. The IPCE, as high as 49%, stems from the effective combination with the acceptor [43]. The photovoltaic properties of devices that include **P1** or **P2** as active layers are presented in Table 4.

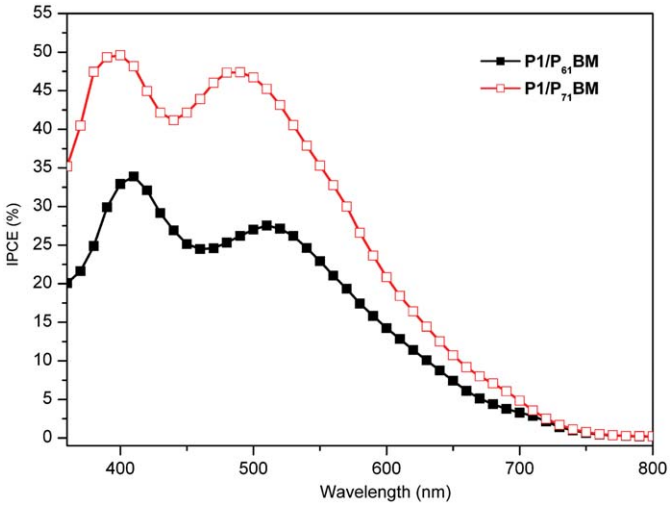

Fig. 5. Comparison of IPCE between the photovoltaic cells based on **P1**/$PC_{61}BM$ and **P1**/$PC_{71}BM$.

Table 4
Photovoltaic characteristics of bulk heterojunctions based on **P1**, **P2**.

Active layer	Thickness (nm)	V_{OC} (V)	J_{SC} (mA/cm^2)	FF	PCE (%)
P1/$PC_{61}BM$ (1:3)	63	0.67	4.46	0.38	1.15
P1/$PC_{71}BM$ (1:3)	58	0.67	6.86	0.37	1.72
P2/$PC_{61}BM$ (1:3)	58	0.07	1.02	0.24	0.017
P2/$PC_{71}BM$ (1:3)	52	0.11	1.68	0.24	0.045

The measurements were carried out at 1000 W m^{-2} and AM 1.5. The structure of the device was: ITO/PEDOT:PSS/pol:PCBM/LiF(7 Å)/Al(120 nm).

4. Conclusion

In conclusion, poly[2,5-bis(thieno-2-yl)-3,6-dipentadecylthieno[3,2-b]thiophene-co-2,1,3-benzothiadiazole] (**P1**) and poly[2,5-bis(3,4-ethylenedioxythieno-2-yl)-3,6-dipentadecylthieno[3,2-b]thiophene-co-2,1,3-benzothiadiazole] (**P2**) were successfully synthesized through the Stille coupling reaction. These polymers were characterized by ^{1}H NMR, GPC, cyclic voltammetry, TGA, and UV–vis spectroscopy. The molecular weights of **P1** and **P2** were not high. It appears that these polymers have rigid chains and poor solubility in organic solvents. Absorption maximas of **P1** and **P2** in the solid film, compared to those in solution, were approximately 70 and 100 nm red shifted, respectively. Shoulder peaks were observed at 678 nm (**P1**) and 738 nm (**P2**), indicating that these polymers have good intermolecular interaction. It is expected that these polymers have relatively high charge mobility properties. The HOMO level of **P1**, as determined by cyclic voltammetry, was 5.17 eV from vacuum, which is lower than the HOMO levels of most regioregular polythiophenes (for example, P3HT, ca. 5.0 eV; poly(3,3‴-didodecyl-quaterthiophene) (PQT-12), ca. 5.1 eV [44]). The best device was obtained with a 58 nm thick active layer of **P1** mixed with $PC_{71}BM$ in the ratio of 1:3, which gave a V_{OC} of 0.67 V, J_{SC} of 6.86 mA/cm^2, and high efficiency of 1.72% under simulated sunlight (1000 W/m^2, AM 1.5). The fill factor, which is the significant factor that limits efficiency, was 0.37, which is considered low and is one of the parameters that must be improved. The photovoltaic property of **P2** was very low, stemming from low molecular weights and unbalanced energy levels with PCBM. Future studies will be carried out to optimize measurement conditions and synthesize **P1** through another synthetic route for increasing the molecular weight.

Acknowledgement

This work was supported by the New and Renewable Energy R&D program (2008-A011-0073) under the Korea Ministry of Knowledge Economy (MKE).

References

[1] T.V. Woudenbergh, J. Wildeman, P.M. Blom, J.A.M. Bastiaansen, B.W. Langeveld-Voss, Electron-enhanced hole injection in blue polyfluorene-based polymer light-emitting diodes, Adv. Funct. Mater. 14 (2004) 677–683.
[2] J. Liu, X. Guo, L. Bu, Z. Xie, Y. Cheng, Y. Geng, L. Wang, X. Jing, F. Wang, White electroluminescence from a single-polymer system with simultaneous two-color emission: polyfluorene blue host and side-chain-located orange dopant, Adv. Funct. Mater. 17 (2007) 1917–1925.
[3] S. Allard, M. Forster, B. Souharce, H. Thiem, U. Scherf, Organic semiconductors for solution-processable field-effect transistors (OFETs), Angew. Chem. Int. Ed. 47 (2008) 4070–4098.
[4] M. Zhang, H.N. Tsao, W. Pisula, C. Yang, A.K. Mishra, K. Müllen, Field-effect transistors based on a benzothiadiazole–cyclopentadithiophene copolymer, J. Am. Chem. Soc. 129 (2007) 3472–3473.
[5] M. Jørgensen, K. Norrman, F.C. Krebs, Stability/degradation of polymer solar cells, Sol. Energy Mater. Sol. Cells 92 (2008) 686–714.
[6] S. Günes, H. Neugebauer, N.S. Sariciftci, Conjugated polymer-based organic solar cells, Chem. Rev. 107 (2007) 1324–1338.
[7] C. Soci, I.W. Hwang, D. Moses, Z. Zhu, D. Waller, R. Gaudiana, C.J. Brabec, A.J. Heeger, Photoconductivity of a low-bandgap conjugated polymer, Adv. Funct. Mater. 17 (2007) 632–636.
[8] F.C. Krebs, M. Jørgensen, K. Norrman, O. Hagemann, J. Alstrup, T.D. Nielsen, J. Fyenbo, K. Larsen, J. Kristensen, Large-area organic photovoltaic module—fabrication and performance, Sol. Energy Mater. Sol. Cells 93 (2009) 422–441.
[9] F.C. Krebs, Polymer solar cell modules prepared using roll-to-roll methods: knife-over-edge coating, slot-die coating and screen printing, Sol. Energy Mater. Sol. Cells 93 (2009) 465–475.
[10] M. Niggemann, B. Zimmermann, J. Haschke, M. Glatthaar, A. Gombert, Organic solar cell modules for specific applications—from energy autonomous systems to large area photovoltaics, Thin Solid Films 516 (2008) 7181–7187.
[11] F.C. Krebs, H. Spanggard, T. Kjær, M. Biancardo, J. Alstrup, Large area plastic solar cell modules, Mater. Sci. Eng. B 138 (2007) 106–111.
[12] H. Hoppe, N.S. Sariciftci, Morphology of polymer/fullerene bulk heterojunction solar cells, J. Mater. Chem. 16 (2006) 45–61.
[13] W. Ma, C. Yang, X. Gong, K. Lee, A. Heeger, Thermally stable, efficient polymer solar cells with nanoscale control of the interpenetrating network morphology, Adv. Funct. Mater. 15 (2005) 1617–1622.
[14] M.C. Scharber, D. Wuhlbacher, M. Koppe, P. Denk, C. Waldauf, A. Heeger, Design rules for donors in bulk-heterojunction solar cells—towards 10% energy-conversion efficiency, Adv. Mater. 18 (2006) 789–794.
[15] J.Y. Lee, W.S. Shin, J.R. Haw, D.K. Moon, Low band gap polymers introduced quinoxaline derivertives and fused thiophene as donor materials for high efficiency bulk-heterojunction type photovoltaic cells, J. Mater. Chem. (2009)10.1039/b823536h.
[16] J. Liu, R. Zhang, G. Sauvé, T. Kowalewski, R.D. McCullough, Highly disordered polymer field effect transistors: n-alkyl dithieno[3,2-b:2′,3′-d]pyrrole-based copolymers with surprisingly high charge carrier mobilities, J. Am. Chem. Soc. 130 (2008) 13167–13176.
[17] E. Bundgaard, F.C. Krebs, Low-band-gap conjugated polymers based on thiophene, benzothiadiazole, and benzobis(thiadiazole), Macromolecules 39 (2006) 2823–2831.
[18] E. Bundgaard, S.E. Shaheen, F.C. Krebs, D.S. Ginley, Bulk heterojunctions based on a low band gap copolymer of thiophene and benzothiadiazole, Sol. Energy Mater. Sol. Cells 91 (2007) 1631–1637.
[19] E. Bundgaard, F.C. Krebs, Large-area photovoltaics based on low band gap copolymers of thiophene and benzothiadiazole or benzo-bis(thiadiazole), Sol. Energy Mater. Sol. Cells 91 (2007) 1019–1025.
[20] B. Xu, S. Holdcroft, Molecular control of luminescence from poly (3-hexylthiophenes), Macromolecules 26 (1993) 4457–4460.
[21] C.R. McNeill, A. Abrusci, J. Zaumseil, R. Wilson, M.J. McKiernan, J.H. Burroughes, J.J.M. Halls, N.C. Greenham, R.H. Friend, Dual electron donor/electron acceptor character of a conjugated polymer in efficient photovoltaic diodes, Appl. Phys. Lett. 90 (2007) 193506-3.
[22] N. Blouin, A. Michaud, M. Leclerc, A low-bandgap poly(2,7-carbazole) derivative for use in high-performance solar cells, Adv. Mater. 19 (2007) 2295–2300.
[23] C. Edder, P.B. Armstrong, K.B. Prado, J.M. Frechet, Benzothiadiazole- and pyrrole-based polymers bearing thermally cleavable solubilizing groups as precursors for low bandgap polymers, J. Chem. Commun. 18 (2006) 1965–1967.
[24] C. Kitamura, S. Tanaka, Y. Yamashita, Design of narrow-bandgap polymers. Syntheses and properties of monomers and polymers containing aromatic-donor and o-quinoid-acceptor units, Chem. Mater. 8 (1996) 570–578.
[25] M. Jayakannan, P.A. van Hal, R.A.J. Janssen, Synthesis and structure–property relationship of new donor–acceptor-type conjugated monomers and

polymers on the basis of thiophene and benzothiadiazole, J. Polym. Sci. A Polym. Chem. 40 (2002) 251–261.
[26] E. Bundgaard, F.C. Krebs, Low band gap polymers for organic photovoltaics, Sol. Energy Mater. Sol. Cells 91 (2007) 954–985.
[27] S.Y. Oh, C.H. Lee, S.H. Ryu, H.S. Oh, Characteristics and fabrication of polymer light emitting diode using copolymer having perylene and triazine moieties in the polymer side chain, J. Ind. Eng. Chem. 12 (2006) 69–75.
[28] S.H. Jin, B.U. Yool, S.Y. Kang, Y.S. Gal, D.K. Moon, Synthesis and electro-optical properties of polythiophene derivatives for electroluminescence display, Opt. Mater. 21 (2003) 153–157.
[29] H. Pang, P.J. Skabara, D.J. Crouch, W. Duffy, M. Heeney, I. McCulloch, S.J. Coles, P.N. Horton, M.B. Hursthouse, Structural and electronic effects of 1,3,4-thiadiazole units incorporated into polythiophene chains, Macromolecules 40 (2007) 6585–6593.
[30] R. Yang, R. Tian, J. Yan, Y. Zhang, J. Yang, Q. Hou, W. Yang, C. Zhang, Y. Cao, Deep-red electroluminescent polymers: synthesis and characterization of new low-band-gap conjugated copolymers for light-emitting diodes and photovoltaic devices, Macromolecules 38 (2005) 244–253.
[31] X. Li, W. Zeng, Y. Zhang, Q. Hou, W. Yang, Y. Cao, Synthesis and properties of novel poly(p-phenylenevinylene) copolymers for near-infrared emitting diodes, Eur. Polym. J. 41 (2005) 2923–2933.
[32] Y. Li, Y. Wu, P. Liu, M. Birau, H. Pan, B.S. Ong, Poly(2,5-bis(2-thienyl)-3,6-dialkylthieno[3,2-b]thiophene)s high-mobility semiconductors for thin-film transistors, Adv. Mater. 18 (2006) 3029–3032.
[33] J.Y. Lee, Y.J. Kwon, J.W. Woo, D.K. Moon, Synthesis and characterization of fluorine.thiophene-based p-conjugated polymers using coupling reaction, J. Ind. Eng. Chem. 14 (2008) 810–817.
[34] K.W. Song, J.Y. Lee, S.W. Heo, D.K. Moon, Synthesis and characterization of a fluorene–quinoxaline copolymer for light-emitting applications, J. Nanosci. Nanotechnol. (2009)10.1166/jnn.2009.1542.
[35] J.L. Bredas, R. Silbey, D.S. Boudreux, R.R. Chance, Chain-length dependence of electronic and electrochemical properties of conjugated systems: polyacetylene, polyphenylene, polythiophene, and polypyrrole, J. Am. Chem. Soc. 105 (1983) 6555–6559.
[36] D.M. deLeeuw, M.M. Simenon, A.B. Brown, R.E.F. Einerhand, Stability of n-type doped conducting polymers and consequences for polymeric microelectronic devices, Synth. Met. 87 (1997) 53–59.
[37] M.S. Liu, X. Jiang, S. Liu, P. Herguth, A.K.Y. Jen, Effect of cyano substituents on electron affinity and electron-transporting properties of conjugated polymers, Macromolecules 35 (2002) 3532–3538.
[38] Y. Liu, M.S. Liu, A.K.Y. Jen, Synthesis and characterization of a novel and highly efficient light-emitting polymer, Acta Polym. 50 (1999) 105–108.
[39] M. Turbiez, P. Frere, M. Allain, C. Videlot, J. Ackermann, J. Roncali, Design of organic semiconductors: tuning the electronic properties of p-conjugated oligothiophenes with the 3,4-ethylenedioxythiophene (EDOT) building block, Chem. Eur. J. 11 (2005) 3742–3752.
[40] C.Q. Ma, M. Fonrodona, M.C. Schikora, M.M. Wienk, R.A.J. Janssen, P. Bauerle, Solution-processed bulk-heterojunction solar cells based on monodisperse dendritic oligothiophenes, Adv. Funct. Mater. 18 (2008) 3323–3331.
[41] W. Tang, L. Ke, L. Tan, T. Lin, T. Kietzke, Z.K. Chen, Conjugated copolymers based on fluorene–thieno[3,2-b]thiophene for light-emitting diodes and photovoltaic cells, Macromolecules 40 (2007) 6164–6171.
[42] Q. Sun, H. Wang, C. Yang, Y. Li, Synthesis and electroluminescence of novel copolymers containing crown ether spacers, J. Mater. Chem. 13 (2003) 800–806.
[43] D. Muhlbacher, M. Scharber, M. Morana, Z. Zhu, D. Waller, R. Gaudiana, C. Brabec, High photovoltaic performance of a low-bandgap polymer, Adv. Mater. 18 (2006) 2884–2889.
[44] B.S. Ong, Y. Wu, P. Liu, S. Gardner, High-performance semiconducting polythiophenes for organic thin-film transistors, J. Am. Chem. Soc. 126 (2004) 3378–3379.